

# Transient Studies of Product Distribution from a Packed Bed Reactor

R. S. KAPNER and H. E. HOELSCHER

The Johns Hopkins University, Baltimore, Maryland

The distribution of reactants and products from a simulated fixed-bed catalytic reactor has been studied. The concentration of both reactant and product in the effluent stream as a function of time has been measured following a sudden change in inlet concentration. The effect of various types and sources of holdup in the bed is discussed. This study is preliminary to further experimental investigations of the mechanism and the rate of exchange of product between a catalyst surface in a fixed-bed reactor and the free stream.

The dynamic equilibrium existing in an on-stream fixed-bed catalytic reactor is the result of a complex relationship among the many processes contributing to the over-all rate. The fluid mechanical or diffusion processes, the adsorption/desorption processes, and the surface phenomena all play important roles. Some advances have been made in this field, notably in those cases where the process is either purely diffusion controlled or entirely dependent upon the rate of the surface reaction. In addition much work has been done on the distribution of mass by diffusion or dispersion in nonreacting fixed beds; a reasonably detailed understanding of this phenomenon has contributed much to the designers skill. Most of this latter effort has been based on considerations of the fixed bed as a mixer. The radial dispersion of materials flowing from a point source has been studied. Longitudinal diffusion studies by frequency response analysis of cyclic inputs have also been made. Transient response techniques have provided information on the residence time distribution of fluid phase holdup and longitudinal diffusion in packed beds. The application of these techniques to the problems arising in chemically reacting systems is still to be realized. This study is intended to explore some aspects of reactor dynamics and specifically to obtain information on distribution and holdup of both products and reactants in an operating reactor.

The system selected for study was the dissolution of metallic zinc in dilute aqueous hydrochloric acid. The approximate equality in observed over-all rates for a wide selection of metals and acids found by Noyes and Whitney (13) and Brunner (3), and the theory developed by Nernst (12) to explain this behavior has been the subject of many research investigations. Bircumshaw and Riddiford (2), Moelwyn-Hughes (11), and Amis (1) in reviewing this theory point up

enough anomalies to jeopardize the wide generality the theory proclaims. Unfortunately most investigators of metal dissolution systems have seemed interested only in checking the Nernst theory and have thrown little light on the surface mechanism of such reactions.

The zinc-hydrochloric acid system was selected for this work because there is a simple stoichiometric relationship in which the number of products is small and well known, the solid could be easily formed into spheres large enough to be packed in a regular array, analysis of trace metals in solution is a thoroughly explored area permitting low levels of reactions, and the heat of reaction is a negligible factor at the low conversions used so that the additional complication of heat transfer at the fluid-solid interface could be neglected.

For these reasons then the dissolution of zinc in dilute hydrochloric acid solution was selected to simulate the general class of fixed-bed catalytic reactions. Although in this system the surface is attacked and removed by the reaction with very dilute acid and hence little total reaction, this factor did not constitute a problem. However it was important that the low concentration used resulted in no hydrogen gas evolution.

## EXPERIMENTAL WORK

The equipment used during this study has been described in detail elsewhere (7, 8), and only a brief description will be given here for the purpose of this paper.

The reaction was studied in a vertical tower of hexagonal cross section packed with zinc spheres in a regular rhombohedral (hexagonal close packing) pattern. This arrangement was chosen to achieve a constant radial void fraction and to obviate questions concerning the packing-geometry and surface-area calculations at a later stage of the work. A schematic of the assembled apparatus showing the tower in position is presented as Figure 1 and a close-up of the working section alone in Figure 2.

A large tank supplied tap water to a centrifugal pump and thence through a control valve and diffuser into a packed flow-straightening section located immediately below the working section. Packing material in the flow-straightening section consisted of inert glass and lucite spheres of approximately  $\frac{1}{2}$ -in. diameter arranged in the same manner as the zinc in the section above. The packed height of the zinc section never exceeded 15 in. Above the working section was a short  $12\frac{1}{2}$ -in. hexagonal section free of packing. A convergent section reducing to  $1\frac{1}{2}$ -in. pipe carried all material to a drain.

Acid resistant materials were used for construction purposes wherever possible. All hexagonal sections, flanges, and the diffuser were built from  $\frac{3}{8}$ -in. sheet lucite. Polyvinyl chloride pipe ( $1\frac{1}{2}$ -in. pipe) was used from the pump exit to the expansion piece. The control valve and the pump impeller and housing were made of bronze. All other piping and the contraction at the top of the tower were made of galvanized iron.

Rubber O rings seated in grooves cut in the lower flange separating any two sections and held in place with 2-in. C clamps provided leak-free gasketing.

The mass flow rate through the tower was measured with interchangeable stainless steel orifice plates located directly above the convergent section. Velocities through the tower were calculated from the mass flow rate and the dimensions of the tower.

It was considered essential that all injected materials entering and leaving the working section be homogeneously distributed. In this way a single sample taken at any radial position, before or after the zinc bed, would be entirely representative of all the fluid in the same place. Prior to packing the reactor with zinc, tracer solutions were injected as point sources from thin tubes placed directly below the diffuser, and samples of solution were taken with a small-bore sampling tube at various radial distances at the exit of the inert packed section. Point values of the tracer concentration were found to be randomly distributed about an average concentration, and the deviation for any one radial sample was never greater than  $\pm 1\frac{1}{2}\%$  for Reynolds numbers greater than 100.

Strong acid solutions for injection into the bulk fluid were made up in 5-gal. glass jars and pumped with nitrogen pressure through a capillary manometer for metering at the injection point. Steady state dissolution data, taken prior to the transient studies, required the addition of potassium nitrate to the acid solution

R. S. Kapner is at Rensselaer Polytechnic Institute, Troy, New York.

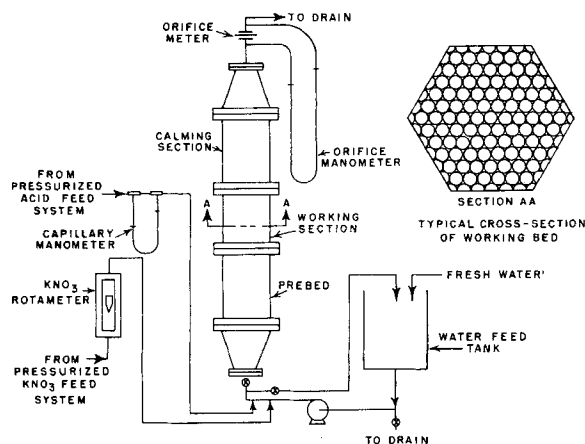


Fig. 1. Reactor assembly and auxiliaries.

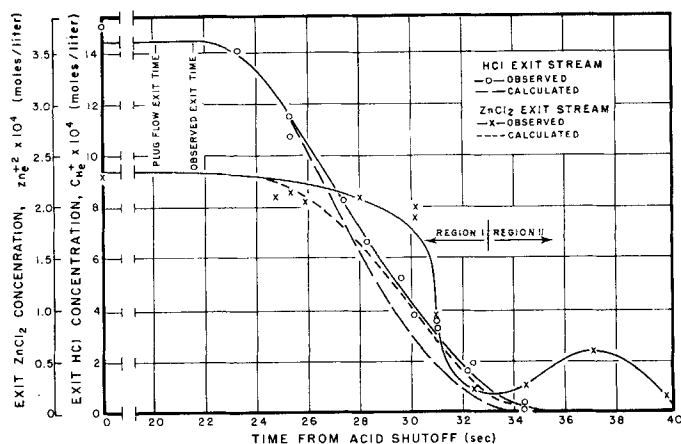


Fig. 3. Product and reaction concentration fall off curves at reactor exit, run T1,  $N_{Re} = 165$ .

flowing to the working section to determine the effect of a depolarizer on the dissolution process. The depolarizer was also pumped with nitrogen pressure from a large glass tank but was metered with a rotameter. Injection of the potassium nitrate into the bulk flow took place at a point slightly upstream from the acid injection point.

The bulk water temperature was measured with an iron-constantan thermocouple located in the discharge pipe above the orifice meter.

Details and characteristics of the packing arrangement are also available elsewhere (4, 7, 10). With the type of packing used the flow path changed direction three times for successively different layers, and this flow pattern was repeated in groups of three layers. As noted the void fraction was constant across the tower radius. The following constants apply:  $\epsilon = 0.27$ ,  $A_s = 150.9$  sq. cm., and  $\alpha = 3.50$  sq. cm./cc.

The zinc used to form the spheres and partial spheres required for the packing was slab zinc of 99.99+ % purity. The average sphere size used was  $0.503 \pm 0.005$  in. The deviation for any single sphere was due more to a lack of sphericity than to variations from sphere to sphere. All spheres, once cast, were tumbled in a ball mill to reduce the mold flash and riser material by attrition. They were then annealed for several hours at 250°F. and allowed to cool slowly to room temperature. The annealing operation was performed to remove the effects of cold working imparted to the spheres in the ball mill. Any grain size would have been suitable as long as it was uniform from sphere to sphere and from the outer surface to the center for any one sphere. Because zinc anneals at room temperature over long periods of time, the crystal structure characteristic of annealed zinc was chosen as the most easily reproducible grain size and one that would not change with time. Microphotographs of an annealed zinc sphere, hand filed to prevent cold working, polished and macroetched with strong hydrochloric acid, showed a uniformly large grain size all the way to the center. This is evidence of the success of the annealing operation. Before the particles in the tower were placed, all

side and corner pieces had their flat sides painted with a clear, tough, unpigmented lacquer (Lin-X gloss varnish) to prevent reaction except on spherical surfaces.

## TRANSIENT PROCEDURE AND RESULTS

### Experimental Procedure

The operating procedure for the study of the dynamic response of the dissolution process consisted of running the reactor under exactly the same conditions as for the steady state (7, 8) and suddenly cutting off the flow of inlet acid. The acid cutoff was accomplished by means of a small-bore glass stopcock in the strong acid injection line. After the system had attained equilibrium at a fixed flow rate, the stopcock was suddenly closed and the system allowed to run down. The history of the concentration fall off of acid in the inlet fluid to the reactor was followed with a conductivity cell in a simple alternating current bridge employing an electronic recorder. The concentration fall off of total ion content in the effluent was followed with a conductivity cell as for the inlet. Exit liquid samples were also taken and

analyzed for acid and zinc. Both these procedures afforded a record of concentration changes. The conductance signals, for the inlet solution, were interpreted entirely in terms of concentration with a previously prepared calibration curve. To accomplish this in situ calibrations were conducted. A conductivity cell was placed just below the working section in the natural interstices of the packing close to one wall. Strong acid solutions were then injected at various rates, and solutions of varying acid strength passed over the cell. A continuous stream of fluid was removed at the same level as the cell and passed to a container devised to permit continuous pH reading. Simultaneous values of recorder scale setting and pH were taken. From this data a calibration of conductance, calculated from bridge values, vs. acid concentration was made. The calibration was found to be a linear relationship between conductance and concentration at the low concentration levels used in this work.

The conductivity cell was made of 0.04-in. diameter platinized platinum,  $\frac{1}{4}$  in. long with about  $\frac{1}{8}$ -in. electrode separation. The two electrodes were insulated from a  $\frac{1}{8}$ -in. I.D. stainless steel tube and cemented firmly in place with a conducting cement.

This calibration procedure did not prove satisfactory for analysis of the exit solutions. It was tried because if successful a combination of exit solution conductance and acid concentration obtained by pH readings on exit samples would have permitted an estimation of the zinc chloride in the transient solutions out of the tower. Unfortunately the low zinc concentration in the exit solutions made such a small contribution to the total conductance that the error involved in this procedure was prohibitive. Effluent conductance was measured but was used only to estimate the time at which concentration decay started in the exit stream. The principal method of determining exit concentrations was by sampling at selected times and analyzing for acid by pH measurement and for zinc by the chemical method developed during the steady state experimental work (7).

The exit liquid samples were taken with a sampling thief (see reference 7 for the design). This sampling tube was placed in the tower just above the zinc

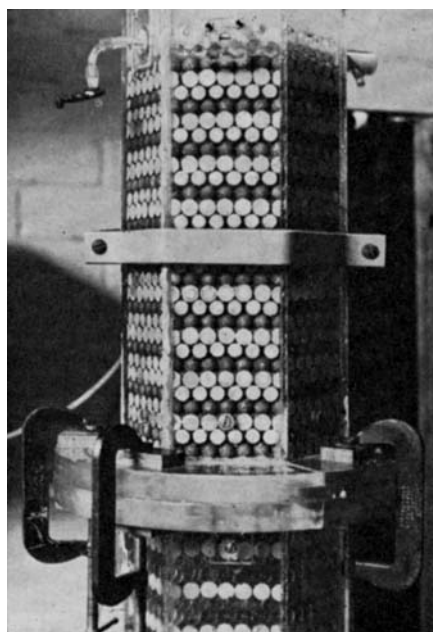


Fig. 2. Close up of zinc-packed working section.

bed. Exit samples were taken at various times from the arbitrary zero defined as that moment at which the inlet acid feed was stopped. Sufficient samples were taken to obtain the transient response curve. These were obtained for both the exit acid and zinc chloride.

#### Data Taken and Results

Transient response data were taken at two widely differing velocities, 1.52 cm./sec. ( $N_{Re} = 165$  at  $14^\circ\text{C.}$ ) and 4.42 cm./sec. ( $N_{Re} = 480$  at  $14^\circ\text{C.}$ ). From the inlet and exit recorder traces, each run being repeated three times, average values of inlet and exit conductance as a function of time were computed. The inlet relationship of concentration to time was immediately calculable from the appropriate calibration curve.

Figures 3 and 4 are the results from the data taken for the two transient runs. In each graph the experimentally determined fall off curves for zinc and acid at the exit of the bed are drawn in solid lines. Each point on these curves is the result of a separate determination. The experimental procedure involved in the use of the sampling thief required that the steady state conditions of acid concentration and flow rate be set up for each sample, the only variation being the time the sample was taken after shutting off the inlet acid. A total of twenty-one separate runs was necessary to define the exit curves for run TI and eighteen runs for TIV.

The two dashed lines shown in these figures represent exit concentrations calculated on the assumption of plug flow, no difference in the diffusional properties of zinc and acid found in the free stream or the boundary layer, and chemical reaction through the tower determined from steady state data for a plane wave of acid passing through the bed. The inlet concentration at any moment was

taken from the inlet acid fall off curve previously measured.

The curves shown are interesting for two reasons: the exit zinc chloride and acid curves show distinctly different concentration-time characteristics from the curves calculated from steady state data, and the initial time for fall off lags considerably behind the time calculated from a simple plug-flow assumption.

#### Steady State Background

An analysis of the data taken for transient runs required some knowledge of the kinetics and mechanism of the steady state dissolution process. A detailed description of the steady state results are available elsewhere (7, 8), but briefly outlined below are some of the more pertinent results of the study, as it relates to transient analysis.

Steady state data were taken for a Reynolds number range of 80 to 700 and an inlet acid concentration range of  $2 \times 10^{-4}$  to  $18 \times 10^{-4}$  moles/liter. Three different bed heights were used, 10.60, 20.97, and 31.34 cm. corresponding to ten, twenty, and thirty layers, respectively, of ordered packing. The transient data reported here corresponds only to the largest bed height and two intermediate Reynolds numbers. The steady state data was correlated with Hoelscher's reactor design equation (5) based upon his characterization of a packed reactor as containing a variable thickness stagnant boundary layer over the solid sphere reaction surface. The equation developed for the steady state runs was

$$f = 1 - \exp \{ 34.80 \times 10^{-4} \times C_{H^+}^{-0.58} \times N_{Re}^{-0.02} \times L \} \quad (1)$$

Equation (1) then was used to calculate the zinc chloride and residual acid concentrations in the reactor effluent

for the transient runs and these values compared with observed transient data. The inlet acid concentration was found from conductivity monitored transient inlet curves for each of the Reynolds numbers used.

A reaction mechanism sequence for the steady state dissolution was developed with the data of Equation (1) and the following assumptions:

1. Over-all rate of reaction is controlled by the diffusion of zinc ions from the reaction surface to the free stream.

2. Hydrogen ions adsorb heavily on the solid zinc reaction surface.

3. Although reaction products (hydrogen gas and zinc ions) might be adsorbed on the surface, they are present in small concentrations compared with adsorbed hydrogen ions.

4. The concentration of hydrogen ions at the reaction interface is equal to the free-stream concentration of this same material.

With these basic assumptions an over-all rate of reaction equation for the rate of zinc production was found to be

$$R_o = \frac{1}{2a} C_{H^+} \left( \frac{df}{d\theta} \right)_{\theta_s} = \frac{2 D_{Zn^{+2}} K_2 N_t (1-f)}{\lambda \delta k_s} \cdot \frac{1}{f} \cdot L \quad (2)$$

where  $K_2$ ,  $\lambda$ , and  $k_s$  are constants for non rate-controlling equilibrium steps. With the data of Equation (1) a correlation of the form suggested by Equation (2) was shown to be valid. Based upon this argument the four assumptions used to develop Equation (2) were also applied to the analysis of transient data.

#### Discussion of Results

Based upon simple material-balance considerations the total moles of acid and zinc chloride leaving the bed as observed from the transient fall off curves should be equal to the total moles leaving the bed when calculated from steady state data. This relationship is obviously not valid for the observed fall off curves. From Figures 3 and 4 it is seen that the areas under the observed exit acid and zinc curves (and hence the masses of material leaving the reactor) are, for both transient runs, greater than the areas for the corresponding calculated curves. Hence more acid and zinc left the bed than was passed into the system during the two transient periods. The mass of excess material for acid and zinc exit streams retained by the bed as a function of time is shown in Figure 5. The ordinate on this graph is defined as

$$F_j(\omega) = U_s A_s \int_{\omega=1}^{\infty} (C_{j\text{obs}} -$$

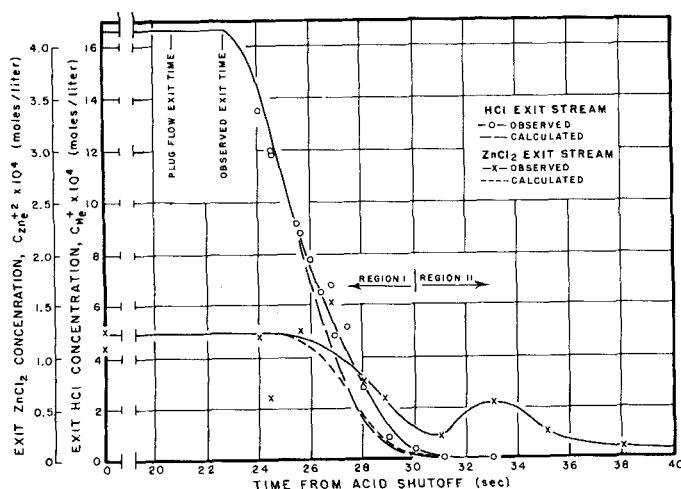


Fig. 4. Product and reaction concentration fall off curves at reactor exit, run TIV,  $N_{Re} = 480$ .

$$C_{j, \text{theo}} d\omega - U_s A_s \int_{\omega=1}^{\omega} (C_{j, \text{obs}} - C_{j, \text{theo}}) d\omega \quad (3)$$

where  $j = H^+$  or  $Zn^{+2}$   
 $\omega = t_e/t_f$

and was evaluated by graphically integrating the exit fall off curves of Figures 3 and 4. The time coordinate has been normalized with respect to the observed time of flight.

To account for the excess material found a mass balance must include sources of acid and zinc other than the feed to the system during the transient period. Two such sources are possible: ions that were adsorbed on bed surfaces before the inlet reactant was cut-off, and ions held up in stagnant fluid regions of the bed.

Two principal regions on Figures 3 and 4 can be seen to contain excess acid and zinc. The first, region I, is that time between the start of fall off and the time most of the acid has left the reactor. During this period the observed exit acid decays smoothly but contains more material than the calculated curves admit to. This holds for the exit zinc fall off curve during the same period of time. Region II concerns only the zinc and occurs after most of the acid has left the bed. This suggests that the zinc appearing in this region is rather unavailable for elution from the reactor. One possible source of zinc ions that could supply the observed excess of Region II is the solid zinc surface. The steady state operation of the bed has previously been characterized as containing an equilibrium concentration of adsorbed hydrogen and zinc ions.

To check the assumption that the zinc mass under the peaked area is due to adsorbed zinc ions, a theoretical amount of adsorbed zinc was computed based upon the assumption that zinc ions are adsorbed on the faces of a zinc crystal equidistant from the atoms constituting the lattice. Zinc crystallizes in hexagonal close-packed array, each cell containing fourteen zinc atoms. In each cell there are six rectangular sides of equal area and two hexagonal surfaces perpendicular to these sides that close the cell. Pearson (14) gives the  $c$  and  $a$  crystal lengths as 4.9368 Å. and 2.6595 Å., respectively. The total area represented by such a cell is  $115.5 \times 10^{-16}$  sq. cm. When one assumes equal opportunity for all cell planes to lie exposed at the surface, this unit area is repeated in integral multiples through the bed. The total surface area for the thirty-layer bed with perfectly smooth particles assumed, is 16,044 sq. cm. If the zinc lattice accommodates one adsorbed zinc ion equidistant from the

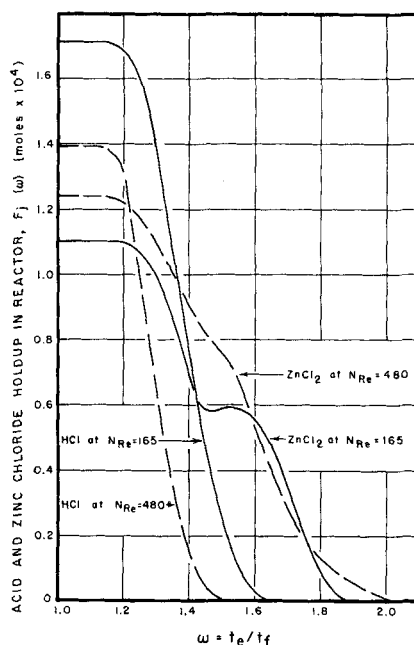


Fig. 5. Reactant and product holdup during transient period, run TI,  $N_{Re} = 165$ ; run TIV,  $N_{Re} = 480$ .

rectangular crystal elements, the unit surface can hold six adsorbed ions, one ion on each rectangular side. Desorbing six zinc ions from a unit area over the entire bed surface represents a total of  $0.14 \times 10^{-4}$  moles of zinc. The mass of zinc represented under the two peaks is  $0.59 \times 10^{-4}$  and  $0.74 \times 10^{-4}$  moles for runs TI and TIV, respectively.

The simple concept of a reversible desorption of zinc ions (see references 7, 8) cannot explain the peaked shape of the zinc fall off curve. This would demand that zinc ions on the surface be strongly dependent on the interfacial concentration of zinc ions in solution. As the acid concentration drops sufficiently to effect the surface rate, this interfacial concentration can no longer be maintained. The concentration of zinc ions at the interface would then decrease as this material diffused to the free stream. The amount of adsorbed zinc would also decrease to maintain a constant ratio of adsorbed to interfacial zinc. The exit zinc curve would then show a continual decrease as material in solution at the interface and adsorbed on the surface moved into the free stream. The shape of the curve would be similar to that of a tracer subjected to a sudden step discontinuity at the inlet to a bed packed with inert porous material. Lapidus (9) shows such fall off curves. The tracer decreases slowly but steadily at the exit of the bed as material diffuses out of the pores into the free stream. Such a process can not result in the peaked-shaped curve.

It is possible to account for this peak if the adsorbed species is subjected to strong surface forces. A drastic reduction in interfacial concentration could then be expected before the surface bond would be broken. The zinc in solution at the solid-fluid interface would then first fall to some low concentration with no measurable decrease in the amount of adsorbed material. After a short time the zinc ion-zinc metal bond would break and the adsorbed zinc diffuse to the free stream, the effect occurring at the bottom of the bed first. As this desorbed zinc passed through the bed, additional material would be released from layers of spheres above the inlet to the reactor. The concentration of zinc in the free stream would build up slowly, but nowhere would the concentration exceed the level at which the surface bond could be broken. In this way a peaked elution curve for adsorbed zinc can be imagined to occur. Two additional observations support this mechanism. First, in both runs the peaks are at about  $0.6 \times 10^{-4}$  moles/liter, suggesting that under different steady state reaction conditions the interfacial zinc concentrations during desorption are probably the same. Second, the ratio of zinc elution times of run TI to run TIV is 2.74 and the ratio of flow rates for these runs is the reciprocal of this, indicating that as surface bonds are broken and zinc reaches the free stream, elution is determined by the free-stream velocity.

Another explanation for the observed excesses is based upon the depletion of material from stagnant bed regions by diffusion as the free-stream concentrations diminish. To check this one may estimate the holdup in such regions and compare this with the observed excess. To make such an estimate it is necessary to propose a simplified model of the bed.

Consider a sphere of radius  $s$ , having a symmetrical zinc chloride concentration layer of thickness  $\delta$ , such that  $C_{zn^{+2}} = C_s$  at  $r = s$  and  $C_{zn^{+2}} = C_m$  at  $r = \delta$ . Under steady state conditions the concentration gradient of zinc is

$$\text{given by the solution to } \frac{d}{dr} \left( r^2 \frac{dc}{dr} \right) = 0 \text{ with the above boundary conditions:}$$

$$C(r) = \frac{sC_s(s + \delta - r) + (s + \delta)C_m(r - s)}{r\delta} \quad (4)$$

The steady state mass flux for a single sphere is

$$M_1 = -4\pi r^2 D \frac{\partial c}{\partial r} \quad (5)$$

Differentiating Equation (4) with re-

spect to  $r$  and substituting the result into Equation (5) one gets

$$M_1 = \frac{4\pi Ds (s + \delta) (C_s - C_m)}{\delta} \quad (6)$$

Equation (6) may be solved for a bed consisting of  $n$  spheres with each sphere assumed to act independently, to yield

$$M_n = n M_1 \frac{4\pi n Ds (s + \delta) (C_s - C_m)}{\delta} \quad (7)$$

The flux rate for the total bed can be evaluated from steady state conversion data with Equation (1):

$$M_n = C_{H^+} \frac{f}{2} U_s A_s \quad (8)$$

To estimate  $C_m$  the average free-stream concentration from inlet to exit can be used. Lapidus (9) provides an estimate of  $\delta$ , the last undetermined variable in Equation (7). With data from the steady state portions of runs TI and TIV, surface concentrations of acid and zinc were evaluated with Equation (7). The stagnant molar holdup of both species were then estimated with the calculated surface concentration; that is holdup mass =  $\delta sLA_s (C_s - C_m)$ .

If this is done the following results are obtained:

Run no.	$N_{Re}$	Holdup material	$C_s$ (calc.)	Molar holdup (predicted)	Molar holdup (observed)
TI	165	ZnCl <sub>2</sub>	$41.7 \times 10^{-4}$	$5.9 \times 10^{-4}$	$0.5 \times 10^{-4}$
		HCl	0	$2.4 \times 10^{-4}$	$1.7 \times 10^{-4}$
TIV	480	ZnCl <sub>2</sub>	$62.4 \times 10^{-4}$	$8.9 \times 10^{-4}$	$0.5 \times 10^{-4}$
		HCl	0	$2.6 \times 10^{-4}$	$1.4 \times 10^{-4}$

The calculated holdups seem to increase with Reynolds number, while the observed holdups are quite constant. This might imply that the observed holdup is independent of throughput or of the amount of reaction. In that case the adsorption phenomenon would be most likely to explain this data.

During the development of the steady state reaction mechanism it was assumed that no hydrogen ion gradient existed through the boundary layer, while the above calculations show the interfacial concentrations to be zero. This discrepancy arises from the method used to calculate the  $H^+$  concentration at the fluid-solid interface. The above calculation assumed that the boundary-layer thickness for both species was the same and that sufficient  $H^+$  must diffuse through this boundary layer to account for the amount of zinc produced. As long as the diffusivity of  $H^+$  is large compared with that of  $Zn^{+2}$ , the actual gradient

of  $H^+$  can act over a much smaller boundary-layer thickness. In that case the assumption of an essentially constant  $H^+$  concentration from free stream to reaction surface is justified. In any case if one assumes no  $H^+$  gradient, the predicted molar holdup for  $H^+$  would be twice the values listed above and no significant change in conclusions would be necessary.

Admittedly the calculations presented above are crude, and the representation of a packed bed as an assemblage of noninteracting particles is not tenable. Further, the assumptions leading to a choice of the concentration boundary layer in a reactor are probably not valid. It is not possible with present data to choose either the adsorption or static volume holdup model as the source of excess acid and zinc. Both possibilities exhibit some merit and seem possible on theoretical grounds. It is quite likely that both sources exist, each providing some of the excess material observed.

The observed time lag in the start of the concentration fall off in the exit stream must also be explained. One possibility is the release of holdup acid from stagnant regions to the free stream. Figures 3 and 4 show the exit time for plug flow ( $L\epsilon/U_s$ ), and the observed time at which the total conductance signal indicated fall off started. For run TI the time lag rep-

resents a 22% increase over the plug-flow time and for run TIV a 50% increase. All available literature indicates that the plug-flow time for non-reacting systems is the maximum time of flight through a packed bed. It is possible that the free stream inlet concentration does fall off before the observed time but that the conductance signal is maintained at or near the steady state value due to diffusion from the boundary-layer regions surrounding the zinc spheres. This possibility, if valid, tends to support the explanation of the zinc fall off based on static volume rather than the argument based upon adsorption.

## CONCLUSION

Most of the literature discussing the Nernst approximation indicates that the rate of a dissolution process is generally a function of velocity and that the process is diffusion controlled. If the Nernst theory is to hold for the dissolution of simple shapes, the sur-

face concentration should be saturated at all velocities or remain constant. In that case increased velocities can produce increased reaction rates as the boundary layer decreases in thickness. From the results reported here the surface concentration of zinc changes from an estimated value of  $42 \times 10^{-4}$  to  $62 \times 10^{-4}$  moles/liter as the velocity increases by a factor of about 3, while the rate of reaction increases by only  $1\frac{1}{2}$  times for this threefold change in velocity. The saturation value for zinc chloride is reported to be 30.8 moles/liter (6). Lapidus (9) also shows that the holdup volume in a packed bed is not a very strong function of velocity. Thus the Nernst approximation seems insufficient.

The question of holdup volume is of particular importance in packed beds. Hoelscher (5) estimated the boundary-layer thickness for the dissolution of zinc in acetic acid from experimental rates over a single cylinder in turbulent flow to be  $8 \times 10^{-4}$  cm. This assumes a first-order reaction and uses the Nernst approximation to calculate  $\delta (= D/k)$ . The rather small boundary-layer thickness, compared with  $9 \times 10^{-3}$  cm. as estimated from Lapidus (9), can be explained by the geometry of a packed bed compared with a single cylinder. In the latter the boundary layer is confined to a thin region covering the surface of the cylinder. A single sphere would also exhibit a similar holdup volume represented by the fluid in viscous motion close to the surface. A packed bed of spheres however contains other sources of holdup volumes, consisting of stagnant fluid regions at points where packing materials are in contact.

It is felt that the application of transient response techniques can be extremely fruitful in studies of reactor dynamics. Much work still remains to be done. For example regions suspected of large holdup can be checked by coating surfaces adjacent to these regions. The concentrations of adsorbed species and their concentration gradients through static boundary layers can be determined for nonionic reactions provided that suitably instantaneous methods of analysis can be found.

In summary then the following is offered:

1. A contribution to understanding the mechanism and kinetics of the zinc-acid dissolution process.
2. Some ideas on product and reactant holdup at and on catalyst surfaces.
3. Evidence that a transient technique such as reported herein may be a powerful tool for reactor dynamic studies.

Of these the last may eventually prove to be most important.

#### ACKNOWLEDGMENT

The authors are appreciative of the interest and suggestions given by W. C. Bastian, for the Metallurgical assistance provided by Mr. Robert Pond and Mrs. Eleanor Harrison, and for the substantial contribution of Mr. Bernard Baker in constructing experimental equipment. R. S. Kapner held the Linde Fellowship in Chemical Engineering for two years of this study and is duly grateful.

#### NOTATION

- $A_s$  = cross-sectional area of empty reactor, sq.cm.  
 $a$  = packed bed surface area per unit of volume, cm.<sup>-1</sup>  
 $C$  = concentration, moles/liter  
 $D$  = molecular diffusivity, sq.cm./sec.  
 $f$  = fractional acid conversion, dimensionless  
 $k$  = first-order reaction velocity constant  
 $L$  = bed height  
 $n$  = number of spheres  
 $M_1$  = mass flux rate for a single reacting sphere, moles/sq.cm.-sec.  
 $N_{Re}$  = Reynolds number based on average particle diameter and

- superficial velocity, dimensionless  
 $N_T$  = molar concentration of surface active sites  
 $R_o$  = over-all rate of reaction, moles/liter sec.  
 $s$  = interfacial condition  
 $t$  = time  
 $t_f$  = time-of-flight (difference between the observed time for the start of concentration fall off at the exit of the bed and the inlet to the bed)  
 $U_s$  = linear velocity based on free cross section, cm./sec.

#### Greek Letters

- $\delta$  = boundary-layer thickness, cm.  
 $\epsilon$  = fraction voids in beds  
 $\omega$  = dimensionless time ratio,  $t_f/t_i$   
 $\lambda$  = constant  
 $\theta$  = time

#### Subscripts

- $f$  = bulk fluid condition  
 $e$  = exit condition  
 $i$  = inlet condition  
 $m$  = mean value across the bed

#### LITERATURE CITED

- Amis, E. S., "Kinetics of Chemical Change in Solution," Macmillan, New York (1949).

- Bircumshaw, L. I., and A. C. Riddiford, *Quart. Chem. Soc.*, **6**, No. 2, p. 157 (1952).
- Brunner, L., *Z. Physik. Chem.*, **35**, 283 (1900).
- Galloway, L. R., W. Komarnicky, and N. Epstein, *Can. J. Chem. Eng.*, **35**, p. 139 (1957).
- Hoelscher, H. E., *A.I.Ch.E. Journal*, **4**, 300 (1958).
- "International Critical Tables," Vol. 4, p. 221, McGraw-Hill, New York (1928).
- Kapner, R. S., Dissertation, Johns Hopkins University, Baltimore, Maryland (1959).
- , and H. E. Hoelscher, *Ind. Eng. Chem.*, **53**, 239 (1961).
- Lapidus, Leon, *ibid.*, **49**, 1,000 (1957).
- Martin, J. J., W. L. McCabe, and C. C. Monrad, *Chem. Eng. Progr.*, **47**, 91 (1951).
- Moelwyn-Hughes, E. A., "The Kinetics of Reactions in Solution," 2 ed., p. 357, Oxford University Press, London, England (1940).
- Nernst, W., "Theoretical Chemistry," 5 ed., p. 669, Macmillan, New York (1923).
- Noyes, A. A., and W. R. Whitney, *Z. Physik. Chem.*, **23**, 689 (1897).
- Pearson, W. B., "Handbook of Lattice Spacings and Structure of Metals and Alloys," p. 886, Pergamon, New York (1958).

Manuscript received October 21, 1960; revision received February 27, 1961; paper accepted February 27, 1961.

# Heterogeneous Phase and Volumetric Behavior of the Methane *n*-Heptane System at Low Temperatures

JAMES P. KOHN

University of Notre Dame, Notre Dame, Indiana

The phase behavior of the methane-*n*-heptane system was determined at temperatures from -200° to 340°F. at pressures up to 1,500 lb./sq. in. abs. The system was found to have a miscibility gap in the liquid-vapor region. The compositions of phases along the three phase ( $L_1$ - $L_2$ - $V$ ) locus indicate that the  $L_1$  phase is approximately 0.64 mole fraction methane and that the  $L_2$  and  $V$  phases are substantially pure methane phases. The quadruple point ( $L_1$ - $L_2$ - $S_1$ - $V$ ) was found at a temperature of -154.4°F. and a pressure of 339 lb./sq. in. abs. A singular point (type  $k$ ) at which the  $L_2$  phase is in critical identity with the vapor phase was found at -114.6°F. and at a pressure of 694 lb./sq. in. abs.

The fugacity of methane at constant temperature as a function of the composition of dissolved methane was found to be linear in the low-temperature range. The plot of Henry's law constant expressed as fugacity mole fraction methane ratio vs. reciprocal absolute temperature was linear in the temperature range from -130° to approximately 100°F. These data indicate that the solution thermodynamics of methane-*n*-heptane is particularly simple in the low-temperature range.

Volumetric and phase behavior of binary hydrocarbon systems have continued to occupy a position of theo-

retical and practical importance. The low-temperature region frequently enables the separation of components which are difficult if not impossible to separate at high temperatures. The present study was undertaken in view of the scarcity of low-temperature

phase and volumetric data on binary hydrocarbon systems.

Mixtures of methane and *n*-heptane have been studied by Boomer (1, 2) who studied mixtures which contained small amounts of nitrogen at pressures up to 3,000 lb./sq. in. abs. and temperatures from 70° to 160°F. An excellent study of mixtures of methane and *n*-heptane was made by Reamer (14) who covered the temperature range from 40° to 460°F. at pressures up to 10,000 lb./sq. in. abs. The Reamer data were compared with the data of the present study, and excellent agreement was obtained.

The volumetric behavior of the pure components has been extensively

Additional data has been deposited as document 6753 with the American Documentation Institute, Photoduplication Service, Library of Congress, Washington 25, D. C., and may be obtained for \$1.25 for photoprints or for 35-mm. microfilm.